Regenerative Therapy 25 (2024) 113–127

Contents lists available at ScienceDirect

Regenerative Therapy

journal homepage: http://www.elsevier.com/locate/reth

Original Article

Simultaneous binding of bFGF to both FGFR and integrin maintains properties of primed human induced pluripotent stem cells

Yu-Shen Cheng [a], Yukimasa Taniguchi [b], Yasuhiro Yunoki [a], Satomi Masai [a], Mizuho Nogi [a], Hatsuki Doi [a], Kiyotoshi Sekiguchi [b], Masato Nakagawa [a, *]

[a] Department of Life Science Frontiers, Center for iPS Cell Research and Application (CiRA), Kyoto University, Kyoto, 606-8507, Japan
[b] Division of Matrixome Research and Application, Institute for Protein Research, Osaka University, Osaka, 565-0871, Japan

ARTICLE INFO

Article history:
Received 3 October 2023
Received in revised form
7 December 2023
Accepted 17 December 2023

Keywords:
Human pluripotent stem cells
bFGF
Integrin
FGFR
Maintenance of pluripotency

ABSTRACT

Introduction: Basic fibroblast growth factor (bFGF, FGF2) and integrin α6β1 are important for maintaining the pluripotency of human pluripotent stem cells (hPSCs). Although bFGF-integrin binding contributes to biofunctions in cancer cells, the relationship in hPSCs remains unclear.
Methods: To investigate the relationship between bFGF and integrin in human induced pluripotent stem cells (hiPSCs), we generated recombinant human bFGF wild-type and mutant proteins, that do not bind to integrin, FGFR, or both. We then cultured hiPSCs with these recombinant bFGF proteins. To evaluate the abilities of recombinant bFGF proteins in maintaining hPSC properties, pluripotent markers, ERK activity, and focal adhesion structure were analyzed through flow cytometry, immunofluorescence (IF), and immunoblotting (IB).
Result: We identified an interaction between bFGF and integrin α6β1 in vitro and in hiPSCs. The integrin non-binding mutant was incapable of inducing the hPSC properties, such as proliferation, ERK activity, and large focal adhesions at the edges of hiPSC colonies. Signaling induced by bFGF-FGFR binding was essential during the first 24 h after cell seeding for maintaining the properties of hPSCs, followed by a shift towards intracellular signaling via the bFGF-integrin interaction. The mixture of the two bFGF mutants also failed to maintain hPSC properties, indicating that bFGF binds to both FGFR and integrin.
Conclusion: Our study demonstrates that the integrin-bFGF-FGFR ternary complex maintains the properties of hPSCs via intracellular signaling, providing insights into the functional crosstalk between bFGF and integrins in hiPSCs.

1. Introduction

Human pluripotent stem cells (hPSCs), such as human embryonic stem cells (hESCs) and human induced pluripotent stem cells (hiPSCs), have the potential to differentiate into nearly all somatic cell types [1,2]. Human PSCs are valuable tools for regenerative medicine because of their pluripotency and ability to proliferate almost indefinitely. The most crucial criterion for cells used in regenerative medicine is safety. To this end, they must be free of animal-derived components and meet the safety standards required for therapeutic use. There are two common methods of culturing hPSCs: the on-feeder method [2] and the feeder-free method [3,4]. Since the on-feeder culture method uses many animal-derived components, including feeder cells derived from mice and bovine serum used to culture the feeder cells [1,2], feeder-free culture has become more popular not only because of its safety but also the convenience of not having to prepare feeder cells.

Basic fibroblast growth factor (bFGF, FGF2) is one of the growth factors with the ability to maintain pluripotency in the naive-to-primed intermediate and primed states of hPSCs [3,5,6]. bFGF activates multiple downstream signaling pathways by binding FGF receptors (FGFRs), consisting of FGFR1, 2, 3, and 4 [7]. Regarding downstream pathways activated by FGFR, Ras/Raf/MEK/ERK

Abbreviations: hPSCs, human pluripotent stem cells; hiPSCs, human induced pluripotent stem cells; bFGF, basic fibroblast growth factor; FGFR, FGF receptor; ECM, extracellular matrix; FAK, focal adhesion kinase; FA, focal adhesion; WT, wild-type; MBP, maltose binding protein; ERK, extracellular signal-regulated kinase; IF, immunofluorescence; IB, immunoblotting; ns, not significant.

* Corresponding author.
E-mail address: nakagawa@cira.kyoto-u.ac.jp (M. Nakagawa).

Peer review under responsibility of the Japanese Society for Regenerative Medicine.

https://doi.org/10.1016/j.reth.2023.12.008

signaling regulates pluripotency and proliferation [6,8], while PI3K/AKT signaling controls pluripotency and survival [9]. Notably, FGF signaling also promotes mesoderm formation [10], implying that crosstalk between some other factors and FGF signaling controls the balance between pluripotency and differentiation.

In feeder-free culture systems, laminins and vitronectin are usually used as extracellular matrix (ECM) to coat cell culture plasticware [11,12]. Integrins and associated downstream signaling are activated through binding to such ECMs [13]. For example, integrin α6β1 promotes cell attachment and maintains pluripotency of hPSCs in the feeder-free culture systems coated with laminin-511, 521, or Matrigel as ECMs [4,14,15], and focal adhesion kinase (FAK) is the integrin-associated factor critical in promoting cell attachment, pluripotency, and hPSC colony structure [16,17]. Ras/Raf/MEK/ERK and PI3K/AKT signaling are also downstream of integrins and FGF [13]. Conversely, integrin/FAK signaling was shown to induce cell differentiation [18], thus revealing a complex relationship between integrins and FGF on cell fate determination.

This intricate relationship between growth factors and integrins has been extensively studied in cancer cells [19]. For instance, FGF1 and bFGF directly interact with integrin αvβ3 to enhance angiogenesis and tumorigenesis in cancer cells [20,21]. Although bFGF and integrins are separately required for maintaining hPSC pluripotency, the possibility for crosstalk between bFGF and integrins in hPSCs remains to be determined.

In the present study, we generated wild-type (WT) and mutant recombinant bFGFs that do not bind to either FGFRs or integrins, or both, to investigate the interaction between bFGF and integrin α6β1 in vitro and in hiPSCs. Mutants that do not bind to either FGFRs or integrins failed to maintain hPSC properties. We examined the precise timing during which bFGF is essential and found the first 24 h after seeding to be critical. Notably, the binding of bFGF to integrins was not required during that period. However, bFGF-FGFR and bFGF-integrin interactions were both necessary one day after cell seeding. ERK signaling induced by bFGF-FGFR binding during the first 24 h after cell seeding was essential to maintaining hPSC properties. Furthermore, both bFGF-FGFR and bFGF-integrin binding cooperatively regulated focal adhesion size at the edges of colonies. Unexpectedly, we found that bFGF must bind FGFRs and integrins simultaneously to maintain the properties of hPSCs, suggesting bFGF, FGFRs, and integrin α6β1 may form a ternary complex in hiPSCs. Altogether, our study reveals a dynamic set of interactions between bFGF and both FGFRs and integrin α6β1 necessary for maintaining the properties of hPSCs.

2. Methods

2.1. Cell culture

Human iPSC cell lines 201B7 [1] and 1383D2 [3] were cultured on 0.5 μg/cm^2 iMatrix-511 (NP892-012, Matrixome) in StemFit medium supplemented with bFGF (C solution in AK03 N medium set) (AK03 N, Ajinomoto) for 7 days. Human iPSCs were passaged using a previously reported protocol [3]. For experiments, hiPSCs were cultured as single cells at low density by plating 2.08 × 10^3 live cells/cm^2 on iMatrix-511-coated plates with StemFit medium containing bFGF (AK03 N), without bFGF (w/o bFGF), StemFit medium supplemented with 100 ng/mL (5.8 nM) bFGF (19,155-07, Nacalai Tesque) [5], 350 ng/mL (5.8 nM) maltose binding protein (MBP)-tagged recombinant bFGF (MBP-bFGF) wild type (WT), 350 ng/mL (5.8 nM) MBP-bFGF mutants. Cells were cultured for 7 days unless specified otherwise. Cells were counted using a R1 cell counter (Olympus).

2.2. Synthesis of recombinant bFGF

A DNA fragment encoding amino acid residues 143–288 of bFGF was amplified by PCR from hiPSC cDNA (1383D2) with pENTR1A-bFGF primers (pENTR1A-bFGF FW and pENTR1A-bFGF RV). The bFGF fragment was cloned into the pENTR1A vector (A10462, Thermo Fisher Scientific) by In-Fusion® HD Cloning Kit (639,650, Takara). The bFGF-K125E and bFGF-Y103A/N104E mutants were made by mutagenesis PCR using pENTR1A-bFGF-WT as a template with bFGF-125 primers (bFGF-125 FW and bFGF-125 RV) and bFGF-103/104 primers (bFGF-103/104 FW and bFGF-103/104 RV). The same PCR was performed sequentially to produce the bFGF-Y103A/N104E/K125E mutant. DNA fragments of bFGF WT and mutants were amplified by PCR with pMAL-c5X-bFGF primers (pMAL-c5X-bFGF FW and pMAL-c5X-bFGF RV) and cloned into the pMAL-c5X vector by In-Fusion® HD Cloning Kit. All DNA plasmids were checked by direct sequencing. The PCR primers were designed using the Primer Design tool for the In-Fusion HD Cloning Kit (Takara) or based on Takara's Mutagenesis with In-Fusion Cloning protocol (Table S1). The plasmids of pMAL-c5X-bFGF-WT and mutants were transformed into BL21 *E. coli* (DE3) competent cells (L1195, Promega). The recombinant proteins of MBP-bFGFs were induced by 1 mM IPTG (19,742-94, Nacalai Tesque) and purified by amylose resin (E8021, New England Biolabs). The column was washed with wash buffer (20 mM Tris/HCl (pH 7.6) (35,436-01, Nacalai Tesque), 1 mM EDTA, 1 mM DTT (14,112-52, Nacalai Tesque), 150 mM NaCl) and eluted with elute buffer (20 mM Tris/HCl (pH 7.6), 1 mM EDTA, 1 mM DTT, 150 mM NaCl, 20 mM Maltose monohydrate). The purified protein was passed through a 0.22 μm Millex®-GV Syringe Filter Unit (SLGVJ13SL, Merck Millipore) and stored at −80 °C.

2.3. Synthesis of recombinant human FGFRs D2D3 domain with fragment crystallizable region (rhFGFRs-Fc)

DNA fragments encoding immunoglobulin-like D2 and D3 domains of FGFRs (FGFR D2D3) were amplified by PCR from hiPSC cDNA (1383D2) and cloned into the pSectag2 vector (V90020, Thermo Fisher Scientific) by In-Fusion® HD Cloning Kit. All DNA plasmids were checked by direct sequencing. The primers for cloning of FGFR1 D2D3, FGFR2 D2D3, FGFR3 D2D3, and FGFR4 D2D3 were designed using the Primer Design tool for the In-Fusion HD Cloning Kit (Table S1). A recombinant human FGFRs D2D3 domain with fragment crystallizable region (rhFGFRs-Fc) was produced using the FreeStyleTM 293 Expression System (Thermo Fisher Scientific) and purified from conditioned media using Protein A Sepharose (GE Healthcare). The column was washed with 20 mM Tris-HCl (pH 7.4)/137 mM NaCl without divalent cation (TBS (−)), and bound proteins were eluted with 0.1 M glycine-HCl (pH 2.8) and immediately neutralized with 1 M Tris-HCl (pH 8.0). The purified protein was dialyzed against TBS (−), passed through a 0.22 μm Millex®-GV Syringe Filter Unit (Merck Millipore), and stored at −75 °C.

Protein concentrations of all recombinant products were determined using a Pierce BCA Protein Assay Kit (Thermo Fisher Scientific) using bovine serum albumin (BSA) as a standard.

2.4. Synthesis of recombinant human integrin α6β1

An expression vector for the extracellular domain of the human integrin α6 subunit with an ACID peptide and a FLAG tag at the C-terminus was prepared as described previously [22]. An expression vector for the extracellular domain of the human integrin β1 subunit with a BASE peptide and a 6 × His tag at the C-terminus was provided by Dr. Junichi Takagi (Institute for Protein Research, Osaka

University) [23]. Recombinant integrin α6β1 was prepared as described previously [24].

2.5. CBB staining and immunoblotting

For Coomassie Blue (CBB) staining, the samples were separated on SDS-PAGE, the gels were washed with Milli-Q water, and stained with Quick-CBB PLUS (178–00551, Wako) for 30 min. To examine ERK and FAK activity, hiPSCs were washed with PBS (14,249-24, Nacalai Tesque) and lysed with a lysis buffer (100 mM Tris/HCl (pH 7.6), 1 % SDS). The samples were adjusted to the same amount, added with SDS sample buffer, and boiled for 10 min. For immunoblotting, the samples were separated on SDS-PAGE, transferred to PVDF membranes (IPVH00010, Immobilon-P, Millipore), and blotted with the following antibodies with iBind Flex system (SLF2000, SLF2010, and SLF2020, Invitrogen): OCT3/4 1:1000 (Anti-Oct4 antibody, Cat. No.: ab19857, Abcam), pERK 1:2000 (Phospho-p44/42 MAPK (Erk1/2) (Thr202/Tyr204), Cat. No.: 4370, CST), ERK 1:1000 (p44/42 MAPK (Erk1/2), Cat. No.: 4695, CST), pFAK 1:1000 (Phospho-FAK (Tyr397), Cat. No.: 44624G, Invitrogen), FAK 1:1000 (Anti-FAK Antibody, clone 4.4, Cat. No.: 05–537, Merck), β-actin 1:2000 (A5441, SIGMA), integrin α6 1:1000 (ab181551, Abcam), FGFR 1:1000 (9740, CST), anti-mouse IgG 1:3000 (7076S, CST), and anti-rabbit IgG 1:1000 (7074S, CST) antibodies.

2.6. Detection and quantification of CBB staining and immunoblotting

CBB-stained gels or immunoblotted membranes were detected by ImageQuant Las 4000 (GE Healthcare) and ImageQuant 800 (Cytiva). Photos were quantified by ImageJ software (NIH). For quantifying the ERK and FAK activity, their activity was calculated as the relative percentage of phosphorylated proteins in the total proteins, and normalized across samples by the amount of actin. The value of fold changes was calculated using day 1 samples cultured with MBP-bFGF-WT as 1.0 and plotted on the graph.

2.7. Solid-phase binding assays

Solid-phase assays for binding of integrin α6β1 and αvβ3 and rhFGFR1-Fc with MBP-bFGF WT and its mutants were carried out as follows. 96-well Nunc MaxiSorp™ flat-bottom plates (Thermo Fisher Scientific) were coated with 50 nM MBP-bFGF-WT, its mutants, or MBP overnight at 4 °C and blocked with blocking solution (TBS containing 0.1 % BSA and 0.02 % Tween 20) for 1 h at room temperature. For integrin binding assays, the plates were incubated with 100 nM integrin α6β1 and integrin αvβ3 for 1 h at room temperature in the presence of 1 mM $MnCl_2$. Bound integrins were detected after sequential incubations with 4.5 μg/mL biotinylated anti-ACID/BASE pAb and 0.53 μg/mL HRP-conjugated streptavidin. The amounts of bound integrins were quantified by measuring absorbance at 490 nm after incubation with o-phenylenediamine and hydrogen peroxide. For the FGFR1-Fc binding assay, the bFGF-coated plate was incubated with 100 nM rhFGFRs-Fc for 1 h at room temperature. Bound rhFGFRs-Fc was detected with 0.4 μg/mL HRP-conjugated anti-human IgG Fc F (ab')2 (Jackson ImmunoResearch Laboratories). The amount of bound rhFGFRs-Fc was quantified by measuring the absorbance at 490 nm after incubation with o-phenylenediamine and hydrogen peroxide. The amounts of recombinant bFGF, its mutants, or MBP adsorbed on the plates were quantified by enzyme-linked immunosorbent assays using anti-MBP mAb (MBL) to confirm the equality of the adsorbed proteins.

A rabbit pAb against the ACID/BASE coiled-coil region was produced as described previously [25]. According to the manufacturer's instructions, the pAb was biotinylated using EZ-LinkTM Sulfo–NHS–LC-Biotin (Thermo Fisher Scientific, Waltham, MA, USA). HRP-conjugated streptavidin was obtained from Thermo Fisher Scientific. HRP-conjugated anti-human IgG Fc F (ab')2 was from Jackson ImmunoResearch Laboratories (West Grove, PA, USA). Anti-MBP mAb was from MBL (Minato-ku, Japan).

2.8. Pull-down assay

Human iPSCs (201B7) cultured for 7 days were lysed in RIPA buffer (20 mM Tris/HCl (pH 7.6) (35,436-01, Nacalai Tesque), 150 mM NaCl (31,320-05, Nacalai Tesque), 0.1 % SDS (31,606-75, Nacalai Tesque), 1 % NP-40 (25,223-75, Nacalai Tesque), 1 mM $MgCl_2$ (20,909, Nacalai Tesque), and protease inhibitor (25,955-11, Nacalai Tesque)). Cell lysates were mixed with amylose resins conjugated with recombinant MBP-tagged bFGF-WT protein and incubated at 4 °C for 1 h. After washing the resins, bound proteins were eluted with SDS sample buffer (125 mM Tris-base (35,434-21, Nacalai Tesque), 960 mM glycine (17,109-35, Nacalai Tesque), and 17.3 mM SDS (31,606-75, Nacalai Tesque)) for immunoblotting.

2.9. Flow cytometry

Cells were harvested with 0.25 % trypsin/1 mM EDTA (25,200-056, Gibco). About 5×10^5 cells were fixed with fixation buffer (420,801, BioLegend) at 37 °C for 15 min. Fixed cells were washed with FACS buffer (2 % FBS, 0.36 % glucose (16,806-25, Nacalai Tesque), 50 μg/μL Pen/Strep in PBS) and permeabilized with 90 % methanol (21,925-05, Nacalai Tesque) at −30 °C overnight. After washing with FACS buffer, the permeabilized cells were stained with the following antibodies in FACS buffer at room temperature for 1 h: BV510-conjugated anti-TRA-1-60 (1:40, 563,188, BD Biosciences) and Alexa Fluor 488 conjugated anti-OCT3/4 (1:5, 560,253, BD Biosciences). Samples were washed with FACS buffer and analyzed by MACSQuant VYB Flow Cytometer (Miltenyi Biotec).

2.10. Immunofluorescence

2.10.1. Triple staining with anti-TRA-1-60 and -OCT3/4 antibodies and Hoechst

Cells were fixed with 4 % formaldehyde (163–20145, Wako) for 15 min at 37 °C. Permeabilization was performed overnight with 90 % methanol (21,925-05, Nacalai Tesque) at −30 °C. Cells were incubated with anti-TRA-1-60 (1:500, 560,071, BD Biosciences) and anti-OCT3/4 (1:500, ab19857, Abcam) antibodies in PBS buffer containing 1 % BSA (01281-84, Nacalai Tesque) for 1 h at room temperature.

2.10.2. Triple staining with anti-phosphorylated and -total ERK (pERK and ERK) and Hoechst

Cells were incubated with 99.8 % methanol at 4 °C for 15 min for fixation and permeabilization. Permeabilized cells were treated with anti-pERK (1:100, 4370, CST) and anti-ERK (1:100, 4696, CST) antibodies in PBS containing 1 % BSA for 1 h at room temperature.

2.10.3. Triple staining with anti-phosphorylated FAK and -total FAK (pFAK and FAK) and Hoechst

The fixation was performed at 37 °C for 15min by 4 % formaldehyde. Cells were permeabilized with PBS containing 0.2 % Triton X-100 (35,501-15, Nacalai Tesque) and 1 % BSA. Cells were stained with anti-pFAK (1:100, 44624G, Thermo Fisher Scientific) and anti-FAK (1:100, 05–537, Merck) antibodies in PBS with 1 % BSA for 1 h at room temperature.

For all staining with secondary antibodies, cells were washed with PBS and stained with the following antibodies in PBS with 1 % BSA: Alexa 488-conjugated goat anti-mouse IgM (1:250, A21042,

Thermo Fisher Scientific), Alexa 488-conjugated goat anti-mouse IgG (H + L) (1:300, A11001, Thermo Fisher Scientific), Alexa 594-conjugated goat anti-rabbit IgG (H + L) (1:300, A11012, Thermo Fisher Scientific), or Hoechst 33,342 (1:1000, 346–07951, Dojindo).

2.11. Imaging and quantification of immunofluorescence

Stained cells were analyzed with a fluorescence microscope (BZ-X710; Keyence).

2.11.1. Quantification of percentages and levels of OCT3/4 expression from IF data

Ten images per well were analyzed by the Hybrid cell counter software (Keyence). Cell numbers were detected by Hoechst staining. The numbers of OCT3/4-positive cells were counted by OCT3/4 staining. The percentages of OCT3/4-positive cells were calculated by the OCT3/4-positive cells/cell numbers ratio. The expression levels of OCT3/4 were determined by the mean fluorescence intensity (MFI) from OCT3/4 staining of every cell in the images.

2.11.2. Quantification of ERK activity from IF data

Ten images per well were analyzed by the Hybrid cell counter software. The areas of cells or colonies were defined by ERK staining, and ERK phosphorylation was detected by pERK staining. ERK activity was determined by comparing the mean of pERK MFI/ERK MFI ratio. The value of fold changes was calculated using day 1 samples cultured with MBP-bFGF-WT as 1.0 and plotted on the graph.

2.11.3. Quantification of the areas of pFAK at the edge of colonies

Ten images per well were analyzed by the ImageJ software (NIH). The quantitation was performed based on a previous study [16]. The areas of pFAK at the edge of colonies were determined by the merged image of pFAK, FAK, and Hoechst (Fig. S7). First, the pFAK, FAK, and Hoechst were separated from the merged image by the "RGB stack" function. (Fig. S7 (1)-(2)). The edges of colonies were determined by the layer of FAK (Fig. S7 (3)). The edge areas were defined as 0.3-inch-thick (1 inch = 36.4 μm) strips by the "Make Band" function, extending 0.2-inch towards the inside and 0.1-inch toward the outside of the edges of colonies (Fig. S7 (4)). The edge area defined by the FAK IF signal was applied to the pFAK layer (Fig. S7 (5)). The pFAK-positive area at the edges of colonies was identified by the "analyze particles" function (Fig. S7 (6)). The means of pFAK-positive areas at the edges of colonies were quantified from 10 colonies per well. The statistics were calculated from 3 independent experiments.

2.12. Statistics

GraphPad Prism (GraphPad Software Inc.)was used for statistics. Data are presented as means ± standard deviation (SD). Unless specified otherwise, no statistically significant differences were detected.

3. Results

3.1. Interaction of bFGF with integrin α6β1

bFGF has been reported to bind to integrins [21], suggesting that it might also activate integrin signaling in hiPSCs. To examine the ability of bFGF to bind to both FGFRs and integrins, we used recombinant bFGF proteins in this study. Maltose binding protein (MBP)-tagged recombinant bFGF (MBP-bFGF) has been commonly used in many studies, including those related to regenerative medicine, protein binding, and cancer therapy [26–29].

To confirm that MBP-bFGF wild type (MBP-bFGF-WT) has a comparable efficacy as commercially available untagged bFGF, we cultivated hiPSCs (clone 201B7) in StemFit AK03 N medium set supplemented with bFGF (AK03 N) [3], StemFit medium with or without 8.3 nM bFGF (100 ng/mL) [5], or with 8.3 nM (350 ng/mL) MBP-bFGF-WT for 7 days and monitored the pluripotency markers, TRA-1-60 and OCT3/4 [30], by flow cytometry (Fig. S1A). While all medium containing bFGF maintained the properties of hPSCs, hiPSCs differentiated when bFGF was absent (w/o bFGF). Human iPSCs cultured with MBP-bFGF-WT formed round and compact colonies, and marker expression was sufficiently high, indistinguishable from AK03 N and bFGF (Fig. S1B and C). The rate of cell proliferation was also similar between hiPSCs cultured with medium containing bFGF (Fig. S1D). These results indicated that MBP-tagged recombinant bFGF was functional.

Integrin α6β1 is the most important integrin and is mainly responsible for maintaining pluripotency in the laminin-511 culture system [12,31]. FGFR1 is the most expressed FGFR in hPSCs [32]. Thus, we focused on bFGF-integrin α6β1 and bFGF-FGFR1 bindings. To identify the interaction between bFGF, integrin α6β1, and FGFR1 in hiPSCs, we performed pull-down assays with MBP-bFGF-WT proteins using hiPSC lysates. As a result, FGFR1 and integrin α6 were detected in the eluates (Fig. 1A). To confirm the direct binding between bFGF and integrins, we tested the binding of MBP-bFGF-WT with recombinant integrin αvβ3 (Fig. 1B) and α6β1 (Fig. 1C) in vitro. The strong binding between integrin αvβ3 and vitronectin, an integrin αvβ3 ligand, was detected. Previous reports have shown that bFGF binds to integrin αvβ3 [21], but we did not observe this interaction in our experiment (Fig. 1B). We verified that MBP-bFGF-WT binds to integrin α6β1 under conditions in which integrin α6β1 binds to iMatrix-511, a known ligand. (Fig. 1C). These results suggest that bFGF specifically binds integrin α6β1 in hiPSCs and directly in vitro.

It was previously reported that Tyr-103/Asn-104 and Lys-125 of bFGF are essential for binding to FGFR [33,34] and integrin αvβ3 [21], respectively. We generated bFGF mutants that do not bind to FGFRs (Y103A/N104A (103/104)), integrins (K125E (125)), or both (Y103A/N104A/K125E (103/104/125)) as recombinant proteins to determine how bFGF binding to FGFRs or integrins affects the properties of hPSCs (Fig. 1D). To characterize these MBP-bFGF mutant proteins, we tested their binding to recombinant FGFRs and integrin α6β1 in vitro. MBP-bFGF-WT bound to all FGFRs, whereas MBP-bFGF-125 only bound to FGFR1, 2, and 4. MBP-bFGF-103/104 showed nearly no binding to FGFR1 and 3, and binding to FGFR2 and 4 was reduced to about half that of MBP-bFGF-WT. MBP-bFGF-103/104/125 did not bind to any FGFRs (Fig. 1E–H). Similarly, we examined the interaction of WT and mutant MBP-bFGFs with integrin α6β1 and observed MBP-bFGF-103/104 to retain binding to integrin α6β1, but both MBP-bFGF-125 and MBP-bFGF-103/104/125 showed reduced interactions (Fig. 1I). These results confirmed Tyr-103/Asn-104 and Lys-125 of bFGF as critical binding sites for FGFR and integrin α6β1, respectively.

3.2. Interaction between bFGF and integrins contributes to hPSC properties

To elucidate the role of the interaction between bFGF and FGFRs or integrins in maintaining the properties of hPSCs, hiPSCs (201B7) were cultured with MBP-bFGF-WT and mutants for 7 days (Fig. 2A) and examined their morphology (Fig. 2B) and assessed pluripotency marker expression via immunofluorescence (IF) and flow cytometry (Fig. 2C and D). Human iPSCs cultured in the absence of bFGF formed flattened and spread-out colonies and showed low

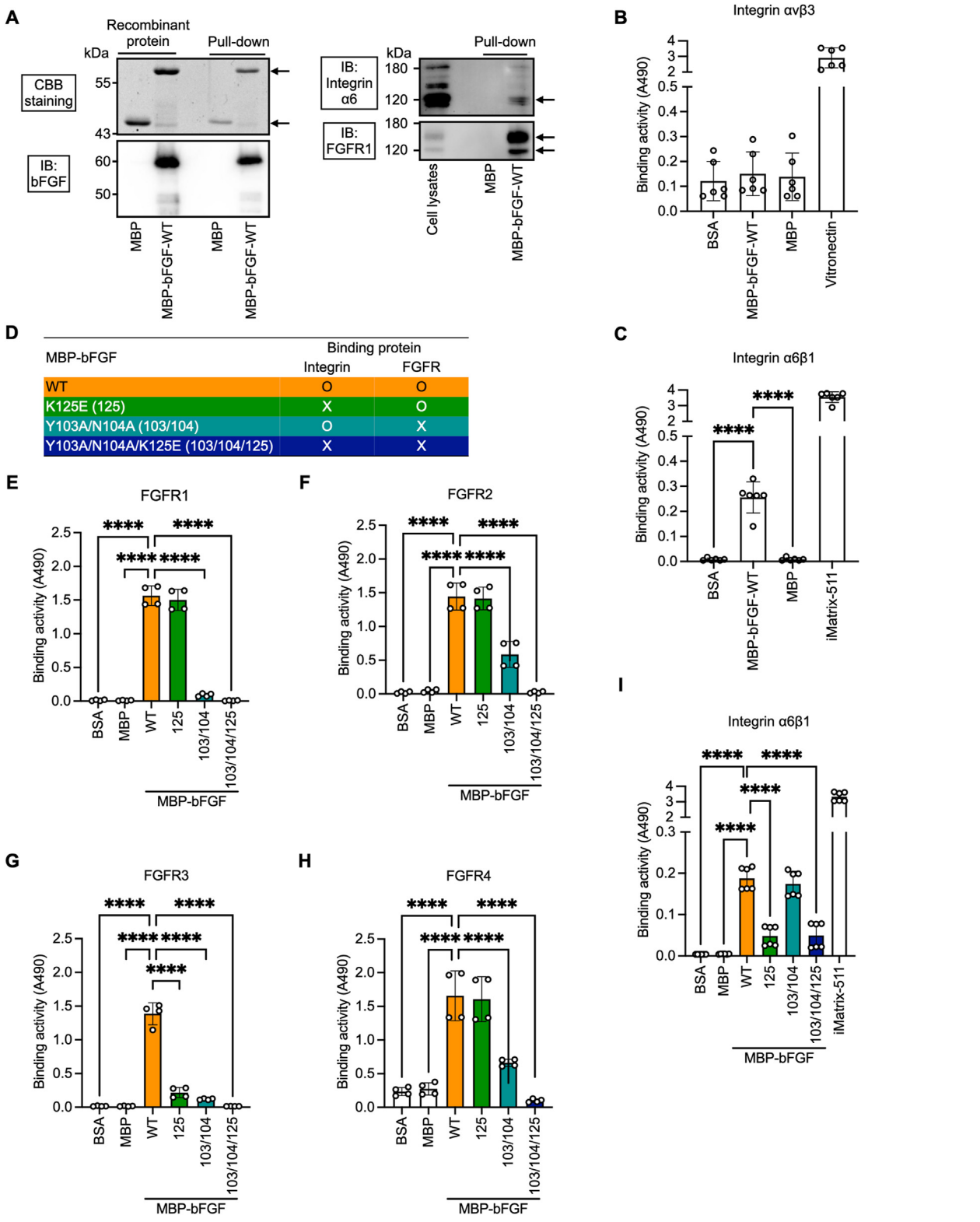

Fig. 1. bFGF binds integrin α6β1 in hiPSCs and in vitro. (A) Pull-down assay using recombinant MBP-bFGF-WT protein. Proteins binding to bFGF were pulled down from the lysates from hiPSCs (201B7) cultured for 7 days. The amount of MBP/MBP-bFGF-WT was confirmed by SDS-PAGE, followed by CBB staining and immunoblotting with anti-bFGF antibody (left images). "Recombinant protein" indicates MBP-tagged proteins before being applied to beads. "Pull-down" indicates proteins after the pull-down assay. The upper and lower arrows at CBB staining indicate the position of MBP-bFGF and MBP, respectively. The binding of bFGF with integrin α6 and FGFR1 was examined by immunoblotting with anti-integrin α6 and -FGFR1 antibodies (right images). Arrows indicate the position of integrin α6 and FGFR1, respectively. (B and C) Results of solid-phase binding assays to confirm the binding of bFGF-WT to integrin αvβ3 (B) or α6β1 (C). Mean (SD) for n = 6 independent experiments, ****p < 0.001, one-way ANOVA with Tukey's test. (D) Summary of information on wild-type (WT) and mutants of MBP-bFGF proteins used in this study. K125E (125) was produced as a mutant that does not bind to integrin, Y103A/N104A (103/104) as a mutant that does not bind to FGFRs, and Y103A/N104A/K125E (103/104/125) as a mutant that does not bind to both FGFRs and integrins. (E–I) Results of solid-phase binding assays to confirm the binding of MBP-bFGF-WT and mutants to FGFR1 (E), FGFR2 (F), FGFR3 (G), FGFR4 (H), or integrin α6β1 (I). Statistical analysis: Mean (SD) for n = 4–6 independent experiments, ****p < 0.0001, **p < 0.01, *p < 0.05, one-way ANOVA with Tukey's test.

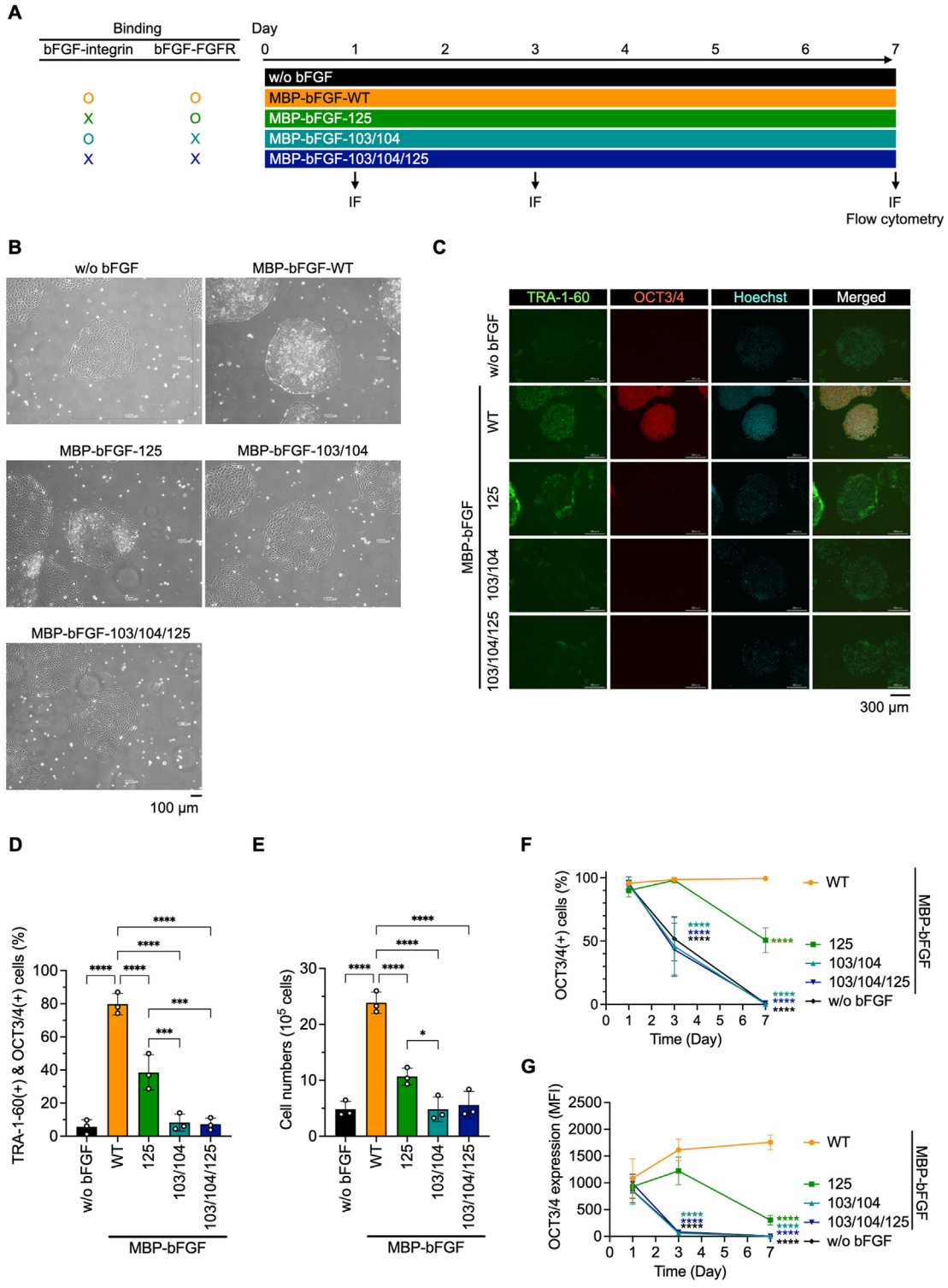

Fig. 2. Binding between bFGF and integrins, as well as FGFRs, maintains hPSC properties. (A) Schematic diagram of the experimental schedule. Human iPSCs (201B7) were cultured for 7 days in medium without bFGF (w/o bFGF) or in medium containing MBP-bFGF-WT, MBP-bFGF-K125E (125), MBP-bFGF-Y103A/N104A (103/104), or MBP-bFGF-Y103A/N104A/K125E (103/104/125). Cell morphology and marker expression analysis by flow cytometry were assessed on day 7, and marker expression analysis by immunofluorescence (IF) was performed on days 1, 3, and 7. (B) Phase contrast images of 201B7 cells with different treatments on day 7 of culture. Scale bar, 100 μm. (C) Immunofluorescence of TRA-1-60 (green), OCT3/4 (red), and Hoechst (cyan) in 201B7 cells on day 7 of culture. Scale bar, 300 μm. (D) Analysis of marker expression by flow cytometry on day 7. The percentages of both TRA-1-60- and OCT3/4-positive cells are shown in the graph. Statistical analysis: Mean (SD) for n = 3 independent experiments, ****p < 0.0001, ***p < 0.001, **p < 0.01, *p < 0.05, one-way ANOVA with Tukey's test. (E) Cell numbers were measured after 7 days of culture. Statistical analysis: Mean (SD) for n = 3 independent experiments, ****p < 0.0001, ***p < 0.001, **p < 0.01, *p < 0.05, one-way ANOVA with Tukey's test. (F) The percentages of OCT3/4-positive cells were quantified from IF data. Statistical analysis: Mean (SD) for n = 3 independent experiments, ****p < 0.0001, ***p < 0.001, **p < 0.01, *p < 0.05, two-way ANOVA, and Dunnett's test. Significant differences compared with WT are indicated. (G) The expression levels of OCT3/4 were quantified from IF data. Statistical analysis: Mean (SD) for n = 3 independent experiments, ****p < 0.0001, ***p < 0.001, **p < 0.01, *p < 0.05, two-way ANOVA, and Dunnett's test. MFI: mean fluorescence intensity. Significant differences compared with WT are indicated.

expression of pluripotent markers TRA-1-60 and OCT3/4 (Fig. 2B–D). When cultured with MBP-bFGF-WT, the colonies were round and compact in shape (Fig. 2B). Cells with MBP-bFGF-WT treatment expressed pluripotent markers at high levels (Fig. 2C and D), and their proliferative capacity was also high (Fig. 2E). When cultured with MBP-bFGF-125, which does not bind integrins readily, cells showed variable morphology in that some remained undifferentiated while others appeared to have undergone differentiation (Fig. 2B). This phenotype was confirmed by measurements of pluripotency markers (Fig. 2C and D) and the cells' proliferative capacity, as they were about half that of MBP-bFGF-WT (Fig. 2E). Pluripotent marker expression and proliferative capacity of hiPSCs treated with MBP-bFGF-103/104 or MBP-bFGF-103/104/125, which do not bind to FGFRs, were similar to those without bFGF (Fig. 2B–E).

Next, time-dependent changes in OCT3/4 expression were analyzed by IF on days 1, 3, and 7 after seeding (Fig. 2A). During the 7-day culture period, MBP-bFGF-WT maintained high expression of OCT3/4 (Fig. 2F and G). Without bFGF, the percentages of OCT3/4-positive cells significantly declined by day 3, and OCT3/4 expression was reduced. MBP-bFGF-125 maintained OCT3/4 expression in most cells, similar to MBP-bFGF-WT, until day 3 but reduced significantly by day 7. MBP-bFGF-103/104 and 103/104/125-treated hiPSCs were similar to those without bFGF treatment. Similar results were obtained with an independent hiPSC line (clone 1383D2) (Fig. S2A–D). These results indicate that the binding of bFGF to integrins and FGFRs plays an important role in maintaining the properties of hPSCs. Notably, the effects of bFGF-integrin binding did not appear immediately after hiPSC seeding but with a delay.

3.3. Importance of bFGF in maintaining hPSC properties immediately after cell seeding

Human iPSCs quickly differentiate without bFGF, suggesting it is constantly required to maintain the properties of hPSCs. To define the critical period during which bFGF is necessary, hiPSCs were collected in medium without bFGF and cultured under several conditions (Fig. 3A). Human iPSCs were cultured for 7 days with (Fig. 3A, #1) or without MBP-bFGF-WT (Fig. 3A, #4). We also cultured cells without bFGF for the first 24 or 48 h after cell seeding and with MBP-bFGF-WT until day 7 (Fig. 3A, #2 and #3, respectively). Conversely, we also cultured hiPSCs with MBP-bFGF-WT for the first 24 h after cell seeding and without bFGF until day 7 (Fig. 3A, #5). After culturing under these different conditions, samples were collected daily from day 1 to day 7 to examine the expression of TRA-1-60 and OCT3/4 by IF. In addition, the expression of OCT3/4 was analyzed by immunoblotting (IB) on day 7 after seeding.

hiPSCs with continuous bFGF treatment for 7 days after seeding formed round and compact colonies with sharp peripheral edges (Fig. 3B #1). By contrast, when cells were cultured without bFGF, colonies became flat and elongated, with cells being dispersed more widely within (Fig. 3B #4). These results were confirmed by IF of TRA-1-60 and OCT3/4 (Fig. 3C). When bFGF was absent during the first 24 h after seeding, cells on day 7 appeared as a mixture of undifferentiated and differentiated cells (Fig. 3B and C #2). In contrast, all cells were differentiated on day 7 when bFGF was absent during the first 48 h after seeding (Fig. 3B and C #3). Notably, when bFGF was present only during the first 24 h after seeding, cells on day 7 had a colony morphology resembling the undifferentiated state (Fig. 3B #5). TRA-1-60 immunofluorescence also indicated an undifferentiated state, although OCT3/4 expression was low (Fig. 3C #5). Furthermore, while the percentages of OCT3/4-positive cells did not decrease when bFGF was added only during the first 24 h after seeding, we observed OCT3/4 levels to decrease (Fig. S3, 3D-3G #5). Altogether, these results indicate bFGF treatment during the first 24 h after seeding is crucial for maintaining the undifferentiated status even though the long-term maintenance of hPSC properties requires the continuous addition of bFGF.

3.4. bFGF-FGFR binding is important immediately after seeding, while bFGF-FGFR and bFGF-integrin interactions are important during the intervening period

Since the function of bFGF during the first 24 h after cell seeding was critical in maintaining undifferentiated hiPSCs, we specifically focused on which interaction is the most important: bFGF-FGFRs, bFGF-integrins, or bFGF-FGFRs-integrins. Human iPSCs were collected without bFGF and seeded in medium with MBP-bFGF-WT or mutants. After 24 h, cells were cultured in medium with MBP-bFGF-WT until day 7, and OCT3/4 expression was examined by IF on days 1, 3, and 7 (Fig. 4A).

When MBP-bFGF-125 was used, colony morphology after 7 days was the same as when hiPSCs were cultured with MBP-bFGF-WT for the entire period (Fig. S4A). OCT3/4 immunofluorescence showed similar results (Fig. 4B, 125-WT and WT-WT). In contrast, when MBP-bFGF-103/104 was used, some but not all cells differentiated (Fig. 4B and S4A, 103/104-WT), similar to when cells were cultured without bFGF during the first 24 h after cell seeding (Fig. 4B and S4A, w/o bFGF-WT). Likewise, cells partially differentiated when MBP-bFGF-103/104/125 was used (Fig. 4B and S4A, 103/104/125-WT).

We also quantified the percentages of OCT3/4-positive cells and the levels of expression by immunofluorescence on days 1, 3, and 7 (Fig. 4C and D). When using MBP-bFGF-WT and the mutant that does not bind integrins (125), the percentages of OCT3/4-positive cells and the expression levels of OCT3/4 were maintained through the entire experimental period (Fig. 4C and D, WT-WT and 125-WT). However, when using the mutants that do not bind to FGFRs (103/104 and 103/104/125), the percentages of OCT3/4-positive cells began to decrease 3 days after seeding (Fig. 4C, 103/104-WT and 103/104/125-WT), similar to hiPSCs without bFGF treatment (Fig. 4C, w/o bFGF-WT). As for the expression levels of OCT3/4, MBP-bFGF-WT and −125 retained high expression throughout, but treatments with other mutants or without bFGF showed a trend for lower expression compared to WT (Fig. 4D). These results indicate that the binding of bFGF to FGFRs on the first day after seeding was essential for maintaining the properties of hPSCs.

Next, we examined the effects of bFGF binding to FGFRs and integrins after the first 24 h. Human iPSCs were seeded in medium with MBP-bFGF-WT for the first day and changed to treatment with MBP-bFGF-WT, mutants, or without bFGF. Colony morphology on day 7 showed a similar appearance under all conditions (Fig. S4B). The expression of OCT3/4 was examined by IF on days 1, 3, and 7 (Fig. 4E). The results showed no change in the percentages of OCT3/4-positive cells under all conditions (Fig. 4F and G). However, significant differences were observed in the expression levels of OCT3/4. When MBP-bFGF-103/104 and −103/104/125 were used or when bFGF was not included in the medium, OCT3/4 expression levels decreased after day 3. When MBP-bFGF-125 was used, OCT3/4 expression also decreased after day 3, but was intermediately between levels of WT and 103/104 or 103/104/125 (Fig. 4F and H). These results indicate that the binding of bFGF to both FGFRs and integrins is required to maintain hPSC properties after the initial 24 h.

3.5. Binding of bFGF to FGFRs and integrins is required for full activation of ERK

Since the binding of bFGF to both FGFRs and integrins during the first day after seeding is critical for maintaining the properties of

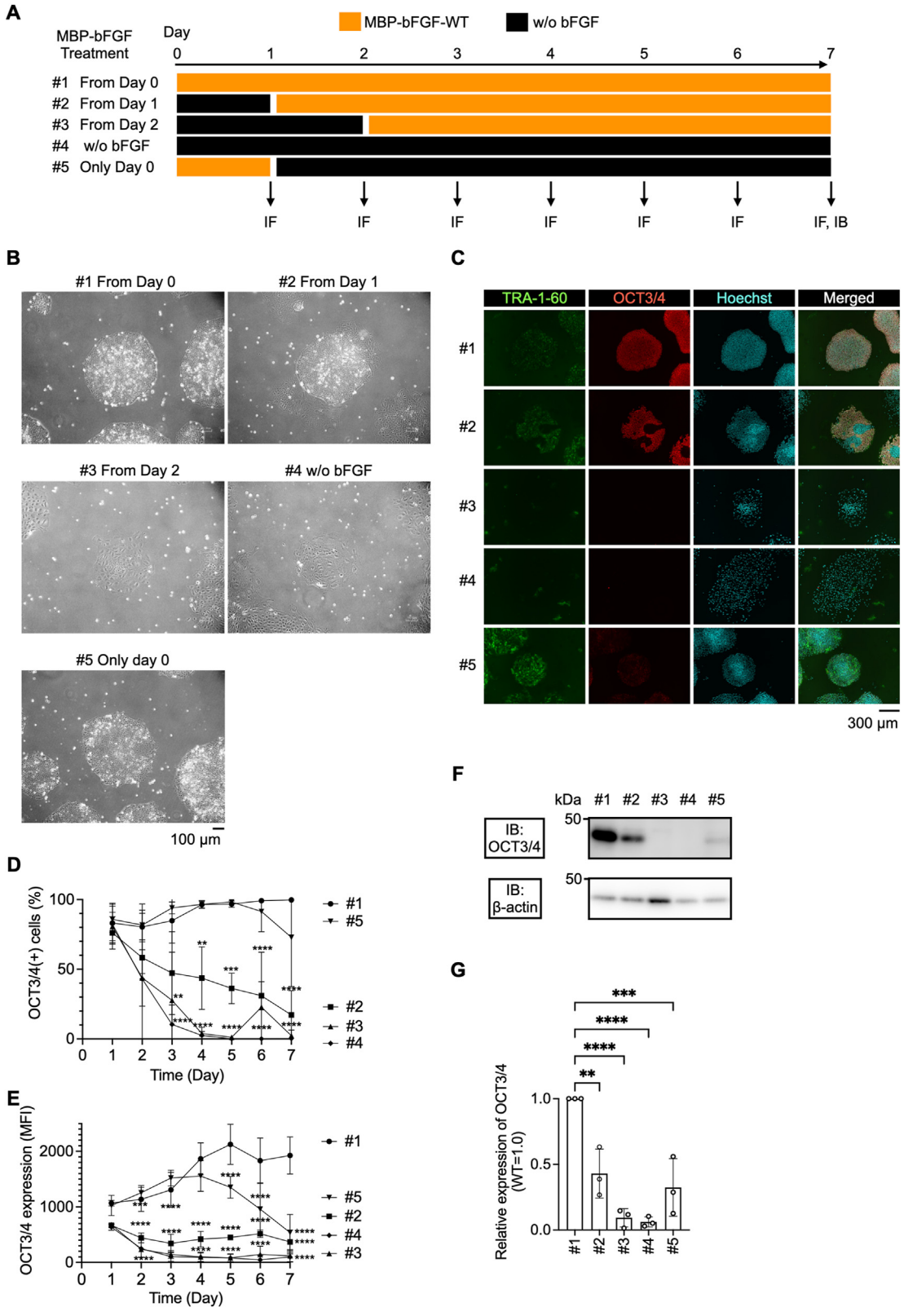

Fig. 3. bFGF treatment during the first 24 h after cell seeding is essential for the maintenance of hPSC properties. (A) Schematic diagram of the experimental schedule. hiPSCs (201B7) were cultured for 7 days with (#1) or without MBP-bFGF-WT (#4). Human iPSCs were cultured without MBP-bFGF-WT for 24 h after cell seeding and from day 1 to day 7 with MBP-bFGF-WT (#2). Cells were cultured without MBP-bFGF-WT for 48 h after cell seeding and from day 2 to day 7 with MBP-bFGF-WT (#3). Cells were cultured with MBP-bFGF-WT for 24 h after cell seeding and from day 1 to day 7 without MBP-bFGF-WT (#5). Samples were collected daily from day 1 to day 7 and analyzed for marker expression by immunofluorescence (IF), and for the expression of OCT3/4 by immunoblotting (IB) on day 7. (B) Phase contrast images of 201B7 cells with different treatments on day 7 of culture. Scale bar, 100 μm. (C) Immunofluorescence of TRA-1-60 (green), OCT3/4 (red), and Hoechst (cyan) in 201B7 cells on day 7 of culture. Scale bar, 300 μm. (D) The percentages of OCT3/4-positive cells were quantified from IF data. Statistical analysis: Mean (SD) for n = 3 independent experiments, ****p < 0.0001, ***p < 0.001, **p < 0.01, *p < 0.05, two-way ANOVA, and Dunnett's test. Significant differences compared with WT are indicated. (E) The expression levels of OCT3/4 were quantified from IF data. Statistical analysis: Mean (SD) for n = 3

hPSCs, we examined the intracellular signals activated by bFGF. ERK (extracellular signal-regulated kinase) is activated downstream of bFGF signaling and supports the maintenance of pluripotency [6,8]. We, therefore, examined ERK activation by immunoblotting (IB) and IF after hiPSCs were cultured with MBP-bFGF-WT or mutants for 24 h (Fig. 5A). When bFGF was not added to the medium, little or no activation of ERK was observed (Fig. 5B, w/o bFGF). When cells were cultured with MBP-bFGF-WT, ERK activation was observed (Fig. 5B, WT). Whereas MBP-bFGF-103/104 and 103/104/125, which do not bind to FGFRs, failed to activate ERK (Fig. 5B, 103/104 and 103/104/125), ERK was only partially activated by MBP-bFGF-125 (Fig. 5B, 125). We also examined the activation of FAK (focal adhesion kinase), previously reported to be associated with the maintenance of pluripotency [17], and found no significant differences (Fig. 5C), potentially due to activation by the binding of integrins to laminins. Furthermore, we observed similar trends of ERK activation on day 1 by immunofluorescence for phosphorylated ERK (Fig. 5D and E). These results together suggest that even though bFGF-integrin binding is crucial to maintaining hPSC properties, only the binding of bFGF to FGFRs could trigger ERK activation.

Since the binding of bFGF with FGFRs and integrins after the first day of seeding is required for maintaining hPSC properties, ERK and FAK activation was also monitored daily by IB during the 7-day period (Fig. S5A–D). When hiPSCs were cultured without bFGF, little activation of ERK was observed during the early culture period. ERK activation increased after day 6 of culture, implying ERK activity might increase with differentiation (Fig. S6A). When hiPSCs were cultured with MBP-bFGF-WT, maximum activation of ERK was observed on day 1 after seeding. From the second day, ERK activation returned to and was maintained at a lower level. When hiPSCs were cultured with MBP-bFGF-125, ERK activation on day 1 was observed but lower than that induced by MBP-bFGF-WT treatment. Following day 2, little, if any, ERK activation was observed. When hiPSCs were cultured with MBP-bFGF-103/104 or −103/104/125, little ERK activation was observed during the early culture period and increased after 6 days in culture. These results were also confirmed by phosphorylated ERK immunofluorescence (Fig. S6A and B). Specifically, high levels of ERK phosphorylation were detected in many cells after day 6 of the culture without bFGF or with MBP-bFGF-103/104 or −103/104/125. Based on cell morphology, ERK activation occurred mostly in differentiated cells. From these observations, we speculate low but continuous ERK activation may be important for maintaining the undifferentiated state of hiPSCs after the initial peak of ERK activation.

3.6. Maintenance of hPSC properties of hiPSCs by binding of bFGF with FGFRs and integrins via FAK activation

Although we did not observe any differences in FAK activation, we examined the relationship between FAK activation and maintenance of hPSC properties from a different perspective. It has been reported that large focal adhesions (FAs) are present at the edges of hiPSC colonies, suggesting FA structures are linked to the pluripotency of hiPSCs [16]. FAK is a key regulator of FA structure and activated FAK co-colocalizes with large FAs at the edges of hiPSC colonies [16,35]. To determine whether the interactions between bFGF and FGFRs or integrins regulate FA structures, hiPSCs were cultured with MBP-bFGF-WT and mutants for 5 days, during which the levels of activated (pFAK: phosphorylated FAK) and total FAK were monitored daily by IF (Fig. 6A and B). Specifically, the area with pFAK in FA sites at the edges of colonies was quantified (Fig. 6C and S7). When hiPSCs were cultured with MBP-bFGF-WT, pFAK accumulated at the edges of colonies on day 2 and remained high throughout the experiment (Fig. 6B and C). When hiPSCs were cultured without bFGF, there was no increase in pFAK. When using MBP-bFGF-125, the accumulation of pFAK at the periphery on day 2 was similar to that observed with MBP-bFGF-WT. However, the size of pFAK decreased after day 3. In contrast, no significant pFAK accumulation was observed at the edges of colonies when MBP-bFGF-103/104 and 103/104/125 were used. These results suggest that the binding of bFGF to FGFRs and integrins regulates the relationship between the accumulation of pFAK at the edge of colonies and hPSC properties.

3.7. Integrin-bFGF-FGFR ternary complex contributes to hPSC properties

Our data indicated bFGF-FGFR and bFGF-integrin interactions contribute to the maintenance of hPSC properties. However, whether those bindings work independently or cooperatively in hiPSCs needs to be clarified. We examined the effects of mixing MBP-bFGF-103/104 and MBP-bFGF-125 on hiPSCs (Fig. 7A). If those interactions function independently, a mixture should maintain hPSC properties. Conversely, if the mixture cannot maintain the properties of hPSCs, simultaneous binding (i.e., they might form a ternary complex) may be required. The results showed that the mixture did not maintain the hPSC properties (Fig. 7B–E and Fig. S8), suggesting that integrin-bFGF-FGFR ternary complex formation potentially contributes to the maintenance of the properties of hPSCs.

4. Discussion

bFGF and integrins are critical factors that maintain the pluripotency of hPSCs in the naive-to-primed intermediate and primed states [6,12,36]. Furthermore, the crosstalk between bFGF and integrins via bFGF-integrin binding was reported in cancer cells [21]. In our study, we found that bFGF can bind to integrin α6β1 and may lead to crosstalk between bFGF and integrin via the formation of an integrin-bFGF-FGFR ternary complex that plays a critical role in maintaining the pluripotency of hiPSCs.

It is commonly believed that bFGF is required constantly for feeder-free long-term hiPSC cultures [3,5]. Our data showed that bFGF is needed immediately after seeding. Surprisingly, hiPSCs treated with bFGF only during the first 24 h after seeding maintained the hPSC properties. However, the pluripotency of the cells cultured with bFGF mutants or without bFGF after 1 day of seeding should be clarified in future studies. These results suggest that bFGF treatment during this early period determines whether cells maintain a pluripotent state or proceed to differentiation.

ERK activation occurs downstream of bFGF for maintaining pluripotency of hPSCs in the naive-to-primed intermediate and primed states [6,8]. Our data showed that ERK activation during the first 24 h after the start of culture is required for maintaining the properties of hPSCs. On the other hand, MBP-bFGF-125 can bind to neither integrins nor FGFR3. Since FGFR3 is not the primary FGFR in hPSCs [32], the reduction of ERK activation in hiPSCs with MBP-bFGF-125 on the first day of cell culture is primarily influenced

independent experiments, ****p < 0.0001, ***p < 0.001, **p < 0.01, *p < 0.05, two-way ANOVA, and Dunnett's test. MFI: mean fluorescence intensity. Significant differences compared with WT are indicated. (F) Immunoblotting (IB) of OCT 3/4 and actin in 201B7 cells on day 7 after seeding. (G) Quantification of the expression levels of OCT3/4 on day 7 from IB data. Statistical analysis: Mean (SD) for n = 3 independent experiments, ****p < 0.0001, ***p < 0.001, **p < 0.01, *p < 0.05, one-way ANOVA with Tukey's test. Significant differences compared with WT are indicated.

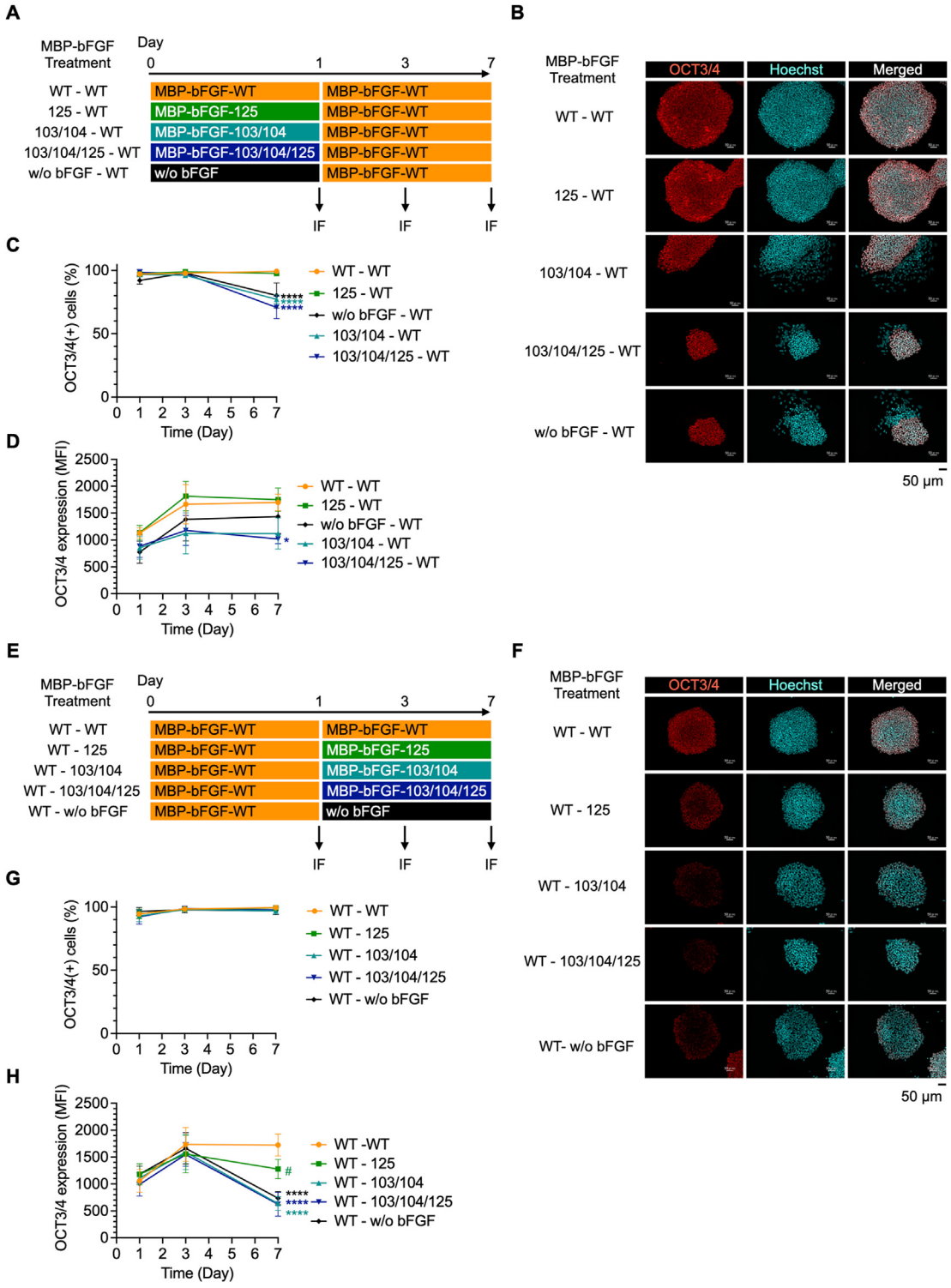

Fig. 4. bFGF-FGFR binding is important immediately after seeding, while bFGF-FGFR and bFGF-integrin interactions are important during the intervening period. (A) Schematic diagram of the experimental schedule. Human iPSCs (201B7) were cultured in medium with MBP-bFGF-WT, −125, −103/104, −103/104/125, or without bFGF for 24 h after seeding and further cultured in medium with MBP-bFGF-WT from day 1 to day 7. Cell morphology was observed on day 7, and marker expression was assessed by immunofluorescence (IF) on days 1, 3, and 7. (B) Immunofluorescence of OCT3/4 (red) and Hoechst (cyan) in 201B7 cells on day 7 of culture. Scale bar, 50 μm. (C) The percentages of OCT3/4-positive cells were quantified from IF data. Statistical analysis: Mean (SD) for n = 3 independent experiments, ****p < 0.0001, ***p < 0.001, **p < 0.01, *p < 0.05, two-way ANOVA, and Dunnett's test. Significant differences compared with WT are indicated. (D) The expression levels of OCT3/4 were quantified from IF data. Statistical analysis: Mean (SD) for n = 3 independent experiments, ****p < 0.0001, ***p < 0.001, **p < 0.01, *p < 0.05, two-way ANOVA, and Dunnett's test. MFI: mean fluorescence intensity. Significant differences compared with WT are indicated. (E) Schematic diagram of the experimental schedule. Human iPSCs (201B7) were cultured in medium with MBP-bFGF-WT for 24 h after seeding and cultured in medium with MBP-bFGF-WT, −125, −103/104, −103/104/125, or without bFGF from day 1 to day 7. Cell morphology was observed on day 7, and marker expression was assessed by IF on days 1, 3, and 7. (F) Immunofluorescence of OCT3/4 (red) and Hoechst (cyan) in 201B7 cells on day 7 of culture. Scale bar, 50 μm. (G) The percentages of OCT3/4-positive cells were quantified from IF data. Statistical analysis: Mean (SD) for n = 3 independent experiments, ****p < 0.0001, ***p < 0.001, **p < 0.01, *p < 0.05, two-way ANOVA, and Dunnett's test. Significant differences compared with WT are indicated. (H) The expression levels of OCT3/4 were quantified from IF data. Statistical analysis: Mean (SD) for n = 3 independent experiments, ****p < 0.0001, ***p < 0.001, **p < 0.01, *p < 0.05, #p = 0.14, two-way ANOVA, and Dunnett's test. Significant differences compared with WT are indicated.

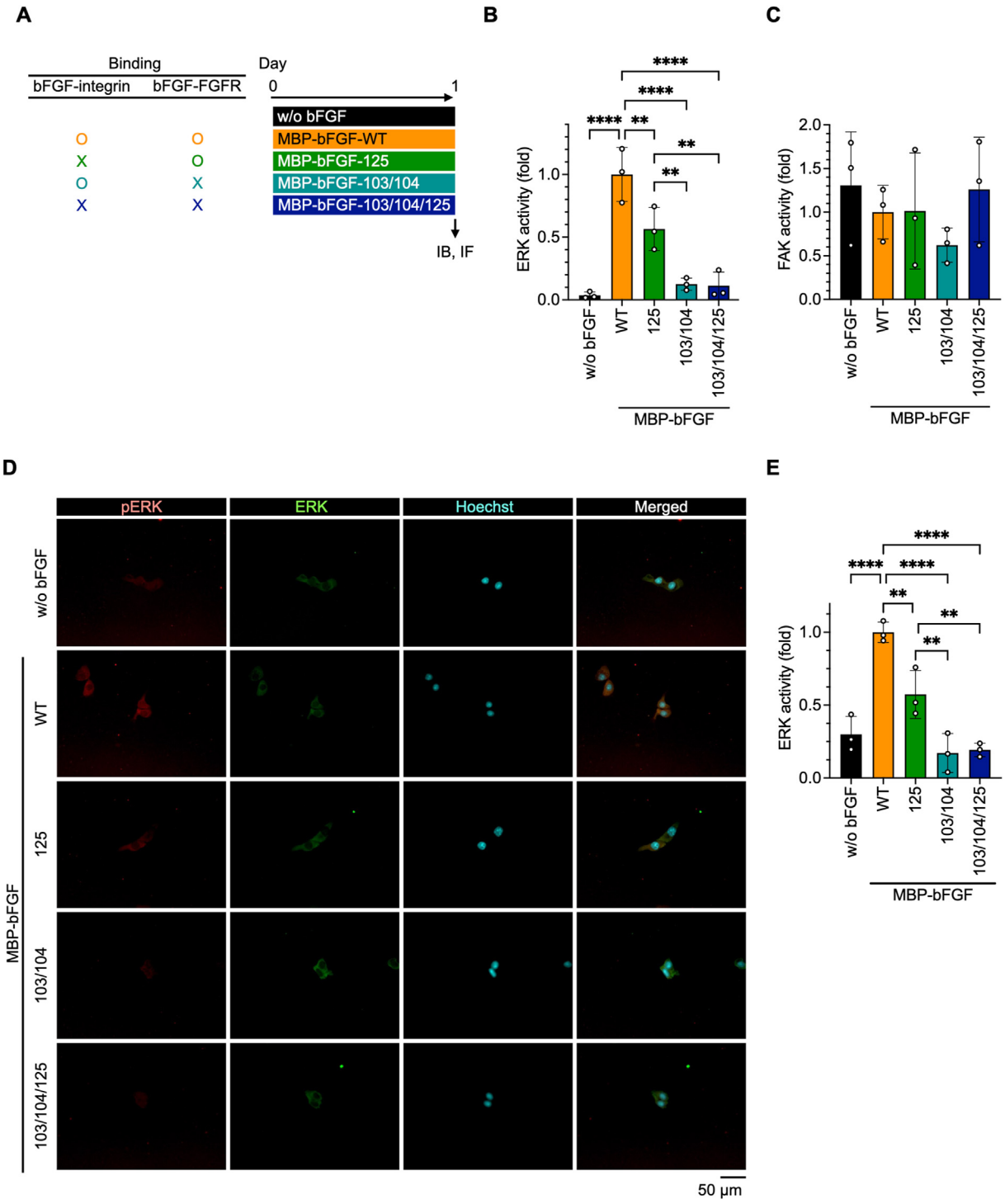

Fig. 5. Binding between bFGF and integrins, as well as FGFRs, contributes to ERK signaling. (A) Schematic diagram of the experimental schedule. Human iPSCs (201B7) were cultured in medium with MBP-bFGF-WT, −125, −103/104, −103/104/125, or without bFGF for 24 h after seeding. On day 1, activation of ERK and FAK was analyzed by immunoblotting (IB) and immunofluorescence (IF). (B) Quantitation of ERK activity on day 1 from IB data. Statistical analysis: Mean (SD) for n = 3 independent experiments, ****p < 0.0001, ***p < 0.001, **p < 0.01, *p < 0.05, one-way ANOVA with Tukey's test. See also Fig. S5A – S5C. (C) Quantitation of FAK activity on day 1 from IB data. Statistical analysis: Mean (SD) for n = 3 independent experiments, ****p < 0.0001, ***p < 0.001, **p < 0.01, *p < 0.05, one-way ANOVA with Tukey's test. See also Fig. S5A – S5B and S5D. (D) Immunofluorescence of phosphorylated ERK (pERK: red), total ERK (ERK: green), and Hoechst (cyan) in 201B7 cells on day 1. Scale bar, 50 μm. See also Fig. S6A. (E) Quantitation of ERK activity from IF data. Statistical analysis: Mean (SD) for n = 3 independent experiments, ****p < 0.0001, ***p < 0.001, **p < 0.01, *p < 0.05, one-way ANOVA with Tukey's test. See also Fig. S6B.

by the lack of bFGF-integrin binding. These findings suggest that the crosstalk between bFGF and integrins activates ERK in hiPSCs. However, further experiments are needed to clarify this issue. There are many pathways to activate ERK: in addition to Ras/Raf/MEK/ERK, Rho family small GTPases, Rac1 and Cdc42, can also activate ERK via the PAK/MAK/ERK signaling pathway [37]. Upstream of ERK, Ras and Rap regulate Raf by different mechanisms [38]. However, since it remains unclear through which pathway the

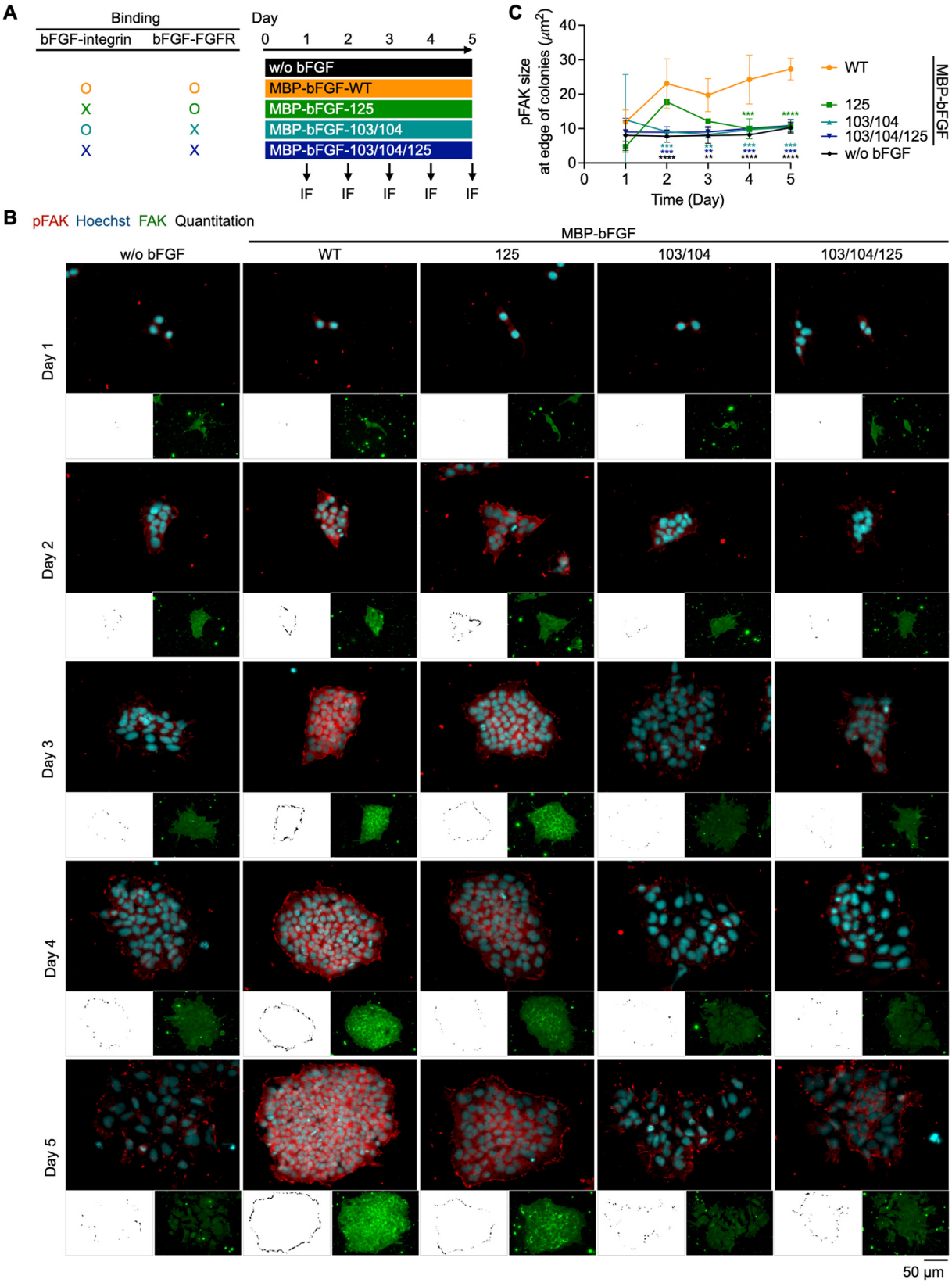

Fig. 6. Binding between bFGF, integrins, and FGFRs regulates focal adhesion structure. (A) Schematic diagram of the experimental schedule. Human iPSCs (201B7) were cultured for 5 days in medium without bFGF (w/o bFGF) or in medium containing MBP-bFGF-WT, MBP-bFGF-K125E (125), MBP-bFGF-Y103A/N104A (103/104), or MBP-bFGF-Y103A/N104A/K125E (103/104/125). Samples were collected daily from day 1 to day 5 and analyzed for FAK activity (phosphorylated FAK, pFAK) by immunofluorescence (IF). (B) Immunofluorescence of phosphorylated FAK (pFAK: red), total FAK (FAK: green), and Hoechst (cyan) in 201B7 cells after 5 days of culture. Representative images of colonies from each treatment group at each time point were used to quantify FAK activity at the edges of colonies (black dots in the inset images). Quantification procedures are described in Fig. S7. Scale bar, 50 μm. (C) The area of accumulated pFAK in the periphery of each colony was quantified from IF data. Statistical analysis: Mean (SD) for n = 3 independent experiments, ****p < 0.0001, ***p < 0.001, **p < 0.01, *p < 0.05, two-way ANOVA, and Dunnett's test. Significant differences compared with WT are indicated.

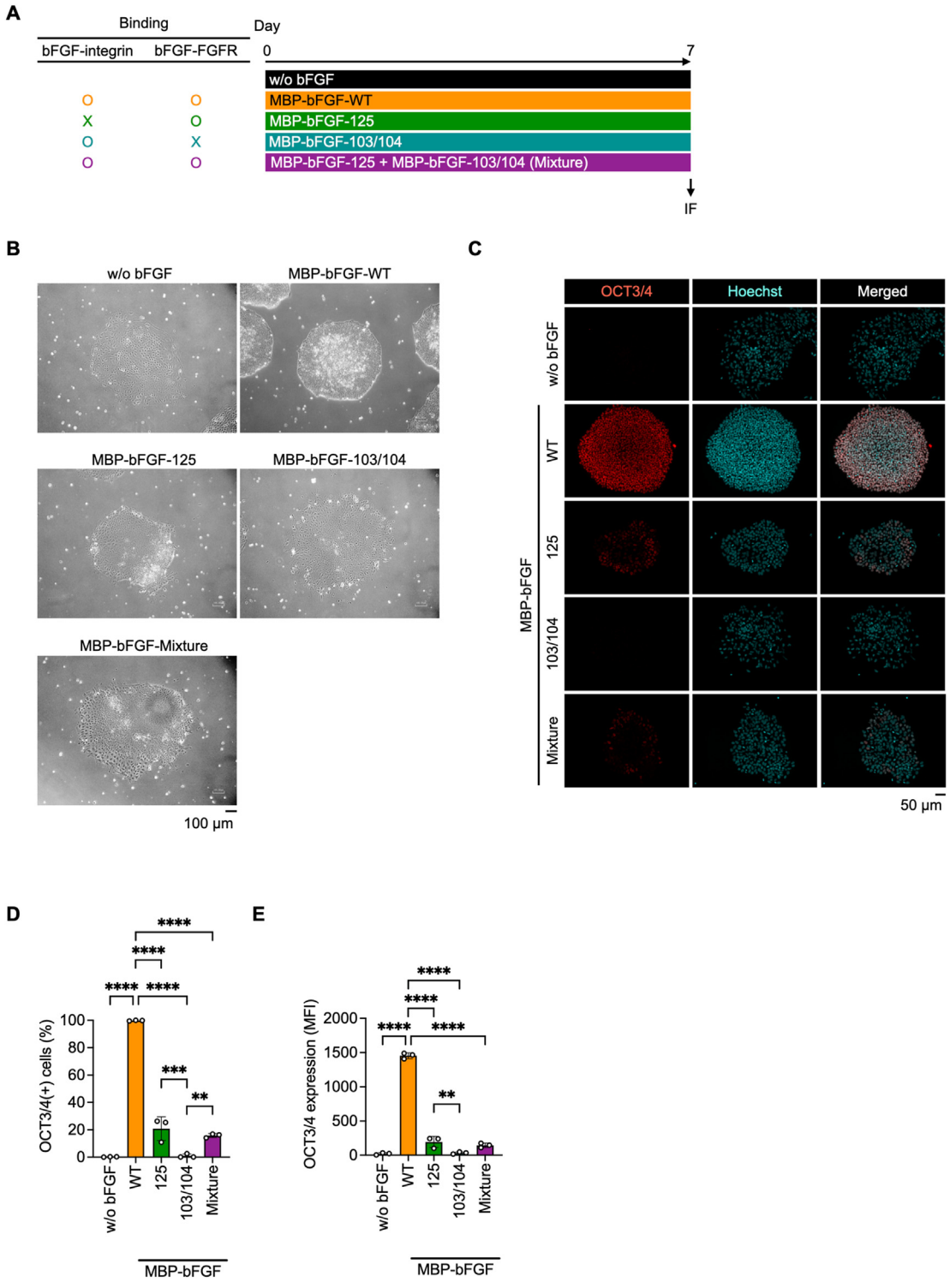

Fig. 7. Importance of integrin-bFGF-FGFR ternary complex for maintaining hPSC properties. (A) Schematic diagram of the experimental schedule. Human iPSCs (201B7) were cultured for 7 days in medium without bFGF (w/o bFGF) or in medium containing MBP-bFGF-WT, MBP-bFGF-K125E (125), MBP-bFGF-Y103A/N104A (103/104), MBP-bFGF-Y103A/N104A/K125E (103/104/125), or a mixture of MBP-bFGF-125 and -103/104 (Mixture). Cell morphology and marker expression analysis by immunofluorescence (IF) were assessed on day 7. (B) Phase contrast images of 201B7 cells with different treatments on day 7 of culture. Scale bar, 100 μm. (C) Immunofluorescence of OCT3/4 (red) and Hoechst (cyan) in 201B7 cells on day 7 of culture. Scale bar, 50 μm. (D) The percentages of OCT3/4-positive cells were quantified from IF data. Statistical analysis: Mean (SD) for n = 3 independent experiments, ****$p < 0.0001$, ***$p < 0.001$, **$p < 0.01$, *$p < 0.05$, one-way ANOVA with Tukey's test. (E) The expression levels of OCT3/4 were quantified from IF data. Statistical analysis: Mean (SD) for n = 3 independent experiments, ****$p < 0.0001$, ***$p < 0.001$, **$p < 0.01$, *$p < 0.05$, one-way ANOVA with Tukey's test.

putative integrin-bFGF-FGFR ternary complex activates ERK, further experiments are necessary to clarify this issue.

On the other hand, although it has been reported that a high level of ERK activity causes hPSCs to differentiate [9], ERK inhibition also causes hPSCs to differentiate [6,8]. These reports indicate a precise level of ERK activation is required to determine hPSC fate. Our results suggest that early ERK activation is essential for maintaining the pluripotent state, and a low ERK activity is subsequently

needed to sustain long-term pluripotency. We speculate that the integrin-bFGF-FGFR complex may help to precisely regulate ERK activation in hiPSCs.

FAK activation regulates cell attachment, pluripotency, and colony structure of hPSCs [16]. Although our data showed that the interaction between bFGF and integrins did not affect FAK activity during the first 24 h after cell seeding, the size of active FAK in the periphery was regulated by the bFGF-integrin binding. As for other factors involved in focal adhesion, Src maintains hiPSCs colony structure by controlling the cytoskeleton, colocalizing with focal adhesions, and phosphorylating FAK at the edges of hPSCs colonies [16]. ERK is also critical in regulating the cytoskeleton and focal adhesions [37]. Because ERK and SRC are downstream of bFGF and integrin signaling, they may regulate FA structures of hiPSC colonies by mediating the crosstalk between bFGF and integrins.

5. Conclusions

We identified the formation of an integrin-bFGF-FGFR ternary complex that might contribute to the maintenance of hPSC properties by regulating ERK activation and focal adhesion size at the edges of hiPSC colonies. Intracellular signaling downstream of ERK activation, possibly activated by bFGF-FGFR binding on the first day of culture, is critical for maintaining the properties of hPSCs, and subsequent intracellular signaling by the integrin-bFGF-FGFR ternary complex is important for maintaining long-term hPSC properties. These findings provide new insight into how crosstalk between integrins, bFGF, and FGFR maintains the properties of hPSCs.

Author contributions

Y. C. and M. N. conceived and wrote the manuscripts. Y. C. mainly prepared all Figures. Y. T. and K. S. supported FGFR and integrin recombinant protein purification and Solid-phase binding assays. All authors supported the completion of the final article.

Declaration of competing interest

K. S. is a co-founder and shareholder of Matrixome, Inc. Y.T. holds a position as a Project Leader at Matrixome Inc.

Acknowledgments

This study was supported by Core Center for iPS Cell Research from Japan Agency for Medical Research and Development (JP21bm0104001) and the iPS Cell Research Fund. We thank Dr. M. Zhao for providing advice about antibodies for IB, Drs. M. Iwasaki, C. Akifuji, T. Imai, and C. Y. Lin for scientific discussions, and Dr. K. Hui for reading the manuscript.

Appendix A. Supplementary data

Supplementary data to this article can be found online at https://doi.org/10.1016/j.reth.2023.12.008.

References

[1] Takahashi K, Tanabe K, Ohnuki M, Narita M, Ichisaka T, Tomoda K, et al. Induction of pluripotent stem cells from adult human fibroblasts by defined factors. Cell 2007;131:861–72. https://doi.org/10.1016/j.cell.2007.11.019.
[2] Thomson JA, Itskovitz-Eldor J, Shapiro SS, Waknitz MA, Swiergiel JJ, Marshall VS, et al. Embryonic stem cell lines derived from human blastocysts. Science 1998;282:1145–7. https://doi.org/10.1126/science.282.5391.1145.
[3] Nakagawa M, Taniguchi Y, Senda S, Takizawa N, Ichisaka T, Asano K, et al. A novel efficient feeder-free culture system for the derivation of human induced pluripotent stem cells. Sci Rep 2014;4:3594. https://doi.org/10.1038/srep03594.
[4] Xu C, Inokuma MS, Denham J, Golds K, Kundu P, Gold JD, et al. Feeder-free growth of undifferentiated human embryonic stem cells. Nat Biotechnol 2001;19:971–4. https://doi.org/10.1038/nbt1001-971.
[5] Chen G, Gulbranson DR, Hou Z, Bolin JM, Ruotti V, Probasco MD, et al. Chemically defined conditions for human iPSC derivation and culture. Nat Methods 2011;8:424–9. https://doi.org/10.1038/nmeth.1593.
[6] Gropp M, Waldhorn I, Gil Y, Steiner D, Turetsky TT, Smith Y, et al. Laminin111-based defined culture promoting self-renewing human pluripotent stem cells with properties of the early post-implantation epiblast. Stem Cell Rep 2022;17:2643–60. https://doi.org/10.1016/j.stemcr.2022.10.010.
[7] Zhang X, Ibrahimi OA, Olsen SK, Umemori H, Mohammadi M, Ornitz DM. Receptor specificity of the fibroblast growth factor family. J Biol Chem 2006;281:15694–700. https://doi.org/10.1074/jbc.M601252200.
[8] Chen G, Gulbranson DR, Yu P, Hou Z, Thomson JA. Thermal stability of fibroblast growth factor protein is a determinant factor in regulating self-renewal, differentiation, and reprogramming in human pluripotent stem cells. Stem Cell 2012;30:623–30. https://doi.org/10.1002/stem.1021.
[9] Singh AM, Reynolds D, Cliff T, Ohtsuka S, Mattheyses AL, Sun Y, et al. Signaling network crosstalk in human pluripotent cells: a smad2/3-regulated switch that controls the balance between self-renewal and differentiation. Cell Stem Cell 2012;10:312–26. https://doi.org/10.1016/j.stem.2012.01.014.
[10] Wardle FC, Smith JC. Transcriptional regulation of mesendoderm formation in Xenopus. Semin Cell Dev Biol 2006;17:99–109. https://doi.org/10.1016/j.semcdb.2005.11.008.
[11] Braam SR, Zeinstra L, Litjens S, Ward-van Oostwaard D, Van Den Brink S, Van Laake L, et al. Recombinant vitronectin is a functionally defined substrate that supports human embryonic stem cell self-renewal via αVβ5 integrin. Stem Cell 2008;26:2257–65. https://doi.org/10.1634/stemcells.2008-0291.
[12] Miyazaki T, Futaki S, Hasegawa K, Kawasaki M, Sanzen N, Hayashi M, et al. Recombinant human laminin isoforms can support the undifferentiated growth of human embryonic stem cells. Biochem Biophys Res Commun 2008;375:27–32. https://doi.org/10.1016/j.bbrc.2008.07.111.
[13] Hynes RO. Integrins: bidirectional, allosteric signaling machines. Cell 2002;110:673–87. https://doi.org/10.1016/S0092-8674(02)00971-6.
[14] Miyazaki T, Futaki S, Suemori H, Taniguchi Y, Yamada M, Kawasaki M, et al. Laminin E8 fragments support efficient adhesion and expansion of dissociated human pluripotent stem cells. Nat Commun 2012;3:1236. https://doi.org/10.1038/ncomms2231.
[15] Rodin S, Antonsson L, Niaudet C, Simonson OE, Salmela E, Hansson EM, et al. Clonal culturing of human embryonic stem cells on laminin-521/E-cadherin matrix in defined and xeno-free environment. Nat Commun 2014;5:3195. https://doi.org/10.1038/ncomms4195.
[16] Närvä E, Stubb A, Guzmán C, Blomqvist M, Balboa D, Lerche M, et al. A strong contractile actin fence and large adhesions direct human pluripotent colony morphology and adhesion. Stem Cell Rep 2017;9:67–76. https://doi.org/10.1016/j.stemcr.2017.05.021.
[17] Vitillo L, Baxter M, Iskender B, Whiting P, Kimber SJ. Integrin-associated focal adhesion kinase protects human embryonic stem cells from apoptosis, detachment, and differentiation. Stem Cell Rep 2016;7:167–76. https://doi.org/10.1016/j.stemcr.2016.07.006.
[18] Villa-Diaz LG, Kim JK, Laperle A, Palecek SP, Krebsbach PH. Inhibition of focal adhesion kinase signaling by integrin α6β1 supports human pluripotent stem cell self-renewal. Stem Cell 2016;34:1753–64. https://doi.org/10.1002/stem.2349.
[19] Eliceiri BP. Integrin and growth factor receptor crosstalk. Circ Res 2001;89:1104–10. https://doi.org/10.1161/hh2401.101084.
[20] Mori S, Wu C-Y, Yamaji S, Saegusa J, Shi B, Ma Z, et al. Direct binding of integrin αvβ3 to FGF1 plays a role in FGF1 signaling. J Biol Chem 2008;283:18066–75. https://doi.org/10.1074/jbc.M801213200.
[21] Mori S, Hatori N, Kawaguchi N, Hamada Y, Shih T-C, Wu C-Y, et al. The integrin-binding defective FGF2 mutants potently suppress FGF2 signalling and angiogenesis. Biosci Rep 2017;37:BSR20170173. https://doi.org/10.1042/BSR20170173.
[22] Ido H, Harada K, Yagi Y, Sekiguchi K. Probing the integrin-binding site within the globular domain of laminin-511 with the function-blocking monoclonal antibody 4C7. Matrix Biol 2006;25:112–7. https://doi.org/10.1016/j.matbio.2005.10.003.
[23] Takagi J, Erickson HP, Springer TA. C-terminal opening mimics 'inside-out' activation of integrin α5β. Nat Struct Biol 2001;8.
[24] Taniguchi Y, Li S, Takizawa M, Oonishi E, Toga J, Yagi E, et al. Probing the acidic residue within the integrin binding site of laminin-511 that interacts with the metal ion-dependent adhesion site of α6β1 integrin. Biochem Biophys Res Commun 2017;487:525–31. https://doi.org/10.1016/j.bbrc.2017.04.051.
[25] Nishiuchi R, Takagi J, Hayashi M, Ido H, Yagi Y, Sanzen N, et al. Ligand-binding specificities of laminin-binding integrins: a comprehensive survey of laminin–integrin interactions using recombinant α3β1, α6β1, α7β1 and α6β4 integrins. Matrix Biol 2006;25:189–97. https://doi.org/10.1016/j.matbio.2005.12.001.
[26] Choi J, Choi W, Joo Y, Chung H, Kim D, Oh SJ, et al. FGF2-primed 3D spheroids producing IL-8 promote therapeutic angiogenesis in murine hindlimb ischemia. Npj Regen Med 2021;6:48. https://doi.org/10.1038/s41536-021-00159-7.
[27] Skjerpen CS, Wesche J, Olsnes S. Identification of ribosome-binding protein p34 as an intracellular protein that binds acidic fibroblast growth factor. J Biol Chem 2002;277:23864–71. https://doi.org/10.1074/jbc.M112193200.
[28] Goodman OB, Febbraio M, Simantov R, Zheng R, Shen R, Silverstein RL, et al. Neprilysin inhibits angiogenesis via proteolysis of fibroblast growth factor-2. J Biol Chem 2006;281:33597–605. https://doi.org/10.1074/jbc.M602490200.

[29] Oh JS, Park IS, Kim KN, Yoon DH, Kim S-H, Ha Y. Transplantation of an adipose stem cell cluster in a spinal cord injury. Neuroreport 2012;23:277–82. https://doi.org/10.1097/WNR.0b013e3283505ae2.
[30] The International Stem Cell Initiative. Characterization of human embryonic stem cell lines by the International Stem Cell Initiative. Nat Biotechnol 2007;25:803–16. https://doi.org/10.1038/nbt1318.
[31] Rodin S, Domogatskaya A, Ström S, Hansson EM, Chien KR, Inzunza J, et al. Long-term self-renewal of human pluripotent stem cells on human recombinant laminin-511. Nat Biotechnol 2010;28:611–5. https://doi.org/10.1038/nbt.1620.
[32] Dvorak P, Dvorakova D, Koskova S, Vodinska M, Najvirtova M, Krekac D, et al. Expression and potential role of fibroblast growth factor 2 and its receptors in human embryonic stem cells. Stem Cell 2005;23:1200–11. https://doi.org/10.1634/stemcells.2004-0303.
[33] Plotnikov AN, Schlessinger J, Hubbard SR, Mohammadi M. Structural basis for FGF receptor dimerization and activation. Cell 1999;98:641–50. https://doi.org/10.1016/S0092-8674(00)80051-3.
[34] Zhu H, Anchin J, Ramnarayan K, Zheng J, Kawai T, Mong S, et al. Analysis of high-affinity binding determinants in the receptor binding epitope of basic fibroblast growth factor. Protein Eng Des Sel 1997;10:417–21. https://doi.org/10.1093/protein/10.4.417.
[35] Mitra SK, Hanson DA, Schlaepfer DD. Focal adhesion kinase: in command and control of cell motility. Nat Rev Mol Cell Biol 2005;6:56–68. https://doi.org/10.1038/nrm1549.
[36] Levenstein ME, Ludwig TE, Xu R-H, Llanas RA, VanDenHeuvel-Kramer K, Manning D, et al. Basic fibroblast growth factor support of human embryonic stem cell self-renewal. Stem Cell 2006;24:568–74. https://doi.org/10.1634/stemcells.2005-0247.
[37] Lavoie H, Gagnon J, Therrien M. ERK signalling: a master regulator of cell behaviour, life and fate. Nat Rev Mol Cell Biol 2020;21:607–32. https://doi.org/10.1038/s41580-020-0255-7.
[38] Raaijmakers JH, Bos JL. Specificity in Ras and Rap signaling. J Biol Chem 2009;284:10995–9. https://doi.org/10.1074/jbc.R800061200.